

A Technique for Estimating the Absolute Gain of a Photomultiplier Tube

M. Takahashi^a, Y. Inome^b, A. Bamba^c, S. Gunjiⁱ, D. Hadasch^a, M.
Hayashida^a, H. Katagiri^f, Y. Konno^g, H. Kubo^g, J. Kushida^h, D. Nakajima^a,
T. Nakamoriⁱ, T. Nagayoshi^j, K. Nishijima^h, S. Nozaki^g, D. Mazin^a, S.
Mashuda^g, R. Mirzoyan^d, H. Ohoka^a, R. Orito¹, T. Saito^a, S. Sakurai^a, J.
Takedaⁱ, M. Teshima^a, Y. Terada^j, F. Tokanaiⁱ, T. Yamamoto^{b,*}, S. Yoshii^b,
T. Yoshida^f

^a*Institute of Cosmic Ray Research, University of Tokyo, Kashiwa, Chiba 277-8582, Japan*

^b*Faculty of Science and Engineering, Konan University, Kobe 658-8501, Japan*

^c*Department of Physics, University of Tokyo, Bunkyo-ku, Tokyo 113-0033, Japan*

^d*Max Planck Institute for Physics, D-80805 Munich Germany*

^e*Institute of Socio- Arts and Science, Tokushima University, Tokushima 770-8502, Japan*

^f*College of Science, Ibaraki University, Mito 310-8512, Japan*

^g*Department of Physics, Kyoto University, Kyoto 606-8502, Japan*

^h*Department of Physics, Tokai University, Hiratsuka, Kanagawa 259-1292, Japan*

ⁱ*Department of Physics, Yamagata University, Yamagata 990-8560, Japan*

¹*Department of Physics, Saitama University, Saitama 338-8570, Japan*

Abstract

Detection of low-intensity light relies on the conversion of photons to photoelectrons, which are then multiplied and detected as an electrical signal. To measure the actual intensity of the light, one must know the factor by which the photoelectrons have been multiplied. To obtain this amplification factor, we have developed a procedure for estimating precisely the signal caused by a single photoelectron. The method utilizes the fact that the photoelectrons conform to a Poisson distribution. The average signal produced by a single photoelectron can then be estimated from the number of noise events, without requiring analysis of the distribution of the signal produced by a single photoelectron. The signal produced by one or more photoelectrons can be estimated experimentally without any assumptions. This technique, and an example of the analysis of a signal from a photomultiplier tube, are described in this study.

*Corresponding author

Email address: tokonatu@konan-u.ac.jp (T. Yamamoto)

Keywords: Photomultiplier, PMT, photoelectron, photon detector

1. Introduction

Light is quantized as photons. If it is very weak, the photons can be counted, which is equivalent to measuring the intensity of the weak light. Since photons are neutral particles, it is difficult to detect them directly. In general, a photon
5 detector converts photons to electrons, which are thus called "photoelectrons." The so-called "quantum efficiency" of a detector is proportional to the efficiency of this conversion from photons to electrons, whereas the overall efficiency of detecting a photon is called the "photo-detection efficiency" [1].

Measurements with high photo-detection efficiency and high precision are
10 important for astronomical observations, such as the Large Size Telescopes in the Cherenkov Telescope Array (CTA)[2]. The goal of the CTA project is to construct the largest observatory of gamma-ray-imaging, atmospheric Cherenkov telescopes, devoted to observations of high-energy photons, with energies ranging from 20 GeV to 300 TeV. The sensitivity in the lowest energy range will
15 be dominated by four LSTs located at the center of the array. To be able to detect low-energy gamma rays, each LST has a large mirror (23 m in diameter) and a high-sensitivity camera. The focal-plane instrument in the camera has to measure weak light with high precision. This requirement brought about the study reported in the present paper.

20 The electrical charge of a photoelectron is 1.6×10^{-19} C. Since this value is extremely small, photoelectrons must be multiplied to be detected as an electrical signal. Photomultiplier tubes (PMTs) are widely used to measure the intensity of such weak light. Photoelectrons are amplified in the PMT and extracted as an electrical signal. Since the amplification is a stochastic process,
25 the electrical signal fluctuates. The fluctuations make the distribution of the signal produced by a single photoelectron wider, depending on the quality of the PMT. In this study, we term the photoelectron signal distribution produced by a single photoelectron "1 PESD." Distributions of two or more photoelectrons

result in the superposition of 1 PESD signals. The number of photoelectrons in
30 a signal can thus be determined by dividing the signal by the average value of
1 PESD, and the number of photons can then be determined from the number
of photoelectrons divided by the photon-detection efficiency. The goal of this
paper is to estimate the average value of a 1 PESD signal.

With the improvement of PMT quality, accurate calibration and quality
35 control become important for experiments such as LST in the CTA. We have
developed a new technique to measure precisely 1 PESD. In this technique,
we first estimate the number of zero-photoelectron events in the data. Then
we estimate 1 PESD through an iteration analysis. Based on this analysis, the
average intensity of the signal produced by a single photoelectron, together with
40 its statistical error, can be estimated from the number of zero-photoelectron
events, and the amplification factor for a single photoelectron can be estimated.
In other words, the amplification factor and its error can be estimated from
the number of noise events, without first determining the value of 1 PESD.
Single and multiple-PESD signals can also be obtained precisely without any
45 ambiguity.

In this paper, we describe in Section 2 the principle of this technique and
demonstrate its use. In Section 3, we discuss and summarize the results.

2. Principle of the Method and Measurements

2.1. Principle of the measurement for a single photoelectron

50 When photoelectrons are ejected from the cathode of a PMT, an electrical
potential of a few hundred volts is applied to attract them to the first dynode.
The number of these primary photoelectrons follows a Poisson distribution [3].
A photoelectron reaching the first dynode has a kinetic energy that depends on
the electrical potential; a voltage of 100 V produces about 5 ~ 10 secondary
55 electrons from the dynode. Some electrons are backscattered from the dynode.
The probability of scattering depends upon the dynode material; for copper, the

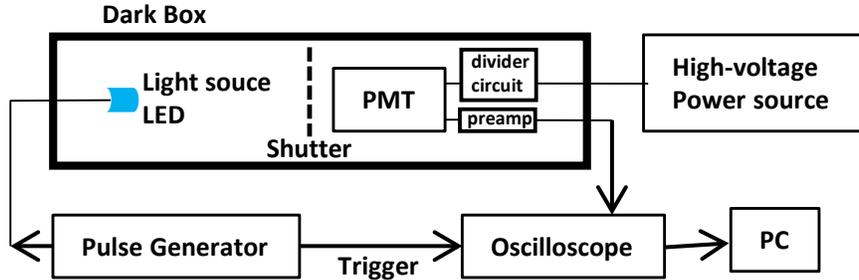


Fig. 1. Schematic view of the experimental setup used to measure 1 PESD. A shutter is placed between the light source and the PMT.

probability is about 27 % [4, 5]. The number of secondary electrons attracted from the first to the second dynode strongly affects the shape of the 1 PESD.

A schematic view of the experimental setup we used to measure 1 PESD is shown in Figure 1. A light-emitting diode (LED) is used as the light source for this measurement. Electrical pulses are sent from a pulse generator to the LED, causing it to emit a weak flash lasting a few nanoseconds. The photons from the LED irradiate the PMT. For our measurements, we used a 1.5-inch PMT (HAMAMATSU R11920-100), which had been developed for the LST in the CTA [6]. The signal from the PMT is amplified by a low-noise preamplifier with a gain of $\times 24$ and is then transferred through a coaxial cable to an instrument such as an oscilloscope [7].

Trigger signals are also sent to the instrument from the pulse generator in order to synchronize the measurement with the LED flash. A typical signal is shown in Figure 2, where the 3 ns pulse width can be clearly seen. The noise level in the signal is a few mV. By integrating the pulse, the signal can be obtained from the charge collected by the PMT anode. The integration time must be wide enough to contain all the signal from the PMT; in the present analysis, we used a 20 ns window. Since longer integration times increase the noise, the duration of the LED flash must be short. Moreover, one must select a PMT with a short pulse-width characteristic.

The distribution of the integrated signal is shown in Figure 3. In this figure,

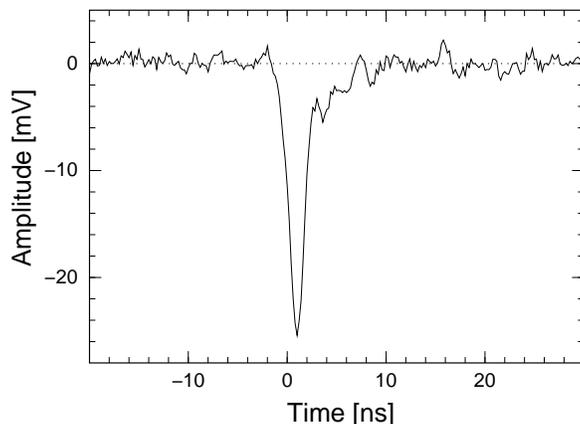


Fig. 2. An example of a signal from the PMT. The signal was amplified by a factor of 24 by the preamplifier and was measured by an oscilloscope with a bandwidth of 300 MHz.

the highest peak occurs around the signal level $q = 0$. No photoelectrons reach the first dynode in these events, which just contain electrical noise. The bump
 80 around $q = 0.8 \text{ pC}$ consists mainly of 1 PESD; i.e., the signal corresponding to a single photoelectron is approximately 0.8 pC . Since the gain of the preamplifier is 24, the amplification factor of the PMT can be estimated approximately as $0.8 \times 10^{-12} \text{ C} / (24 \times 1.6 \times 10^{-19} \text{ C}) \approx 2 \times 10^5$. An accurate measurement of this value and its associated statistical error is the main purpose of the present study.
 85 Events above 1 pC contain two or more photoelectrons. Consequently 1 PESD can be found as the residual after 0 and two or more PESDs are subtracted from all events.

2.2. Poisson distribution of the number of photoelectrons and 0 PESD

In this section, we describe a procedure for estimating 1 PESD from the
 90 data. The goal of this analysis is to estimate 1 PESD and thus determine the amplification factor of the PMT, along with its statistical error.

As indicated in Figure 1, a shutter is located between the LED and the PMT. Two measurements were performed using this shutter: in one, the PMT

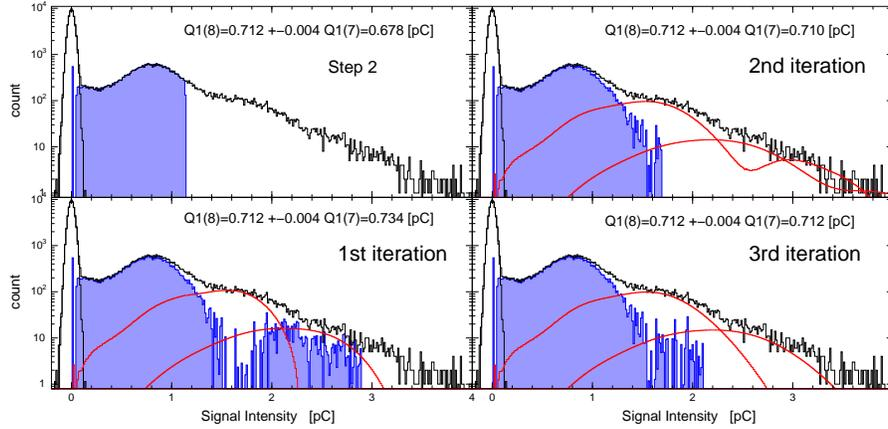


Fig. 3. Distribution of signal from the PMT. A high voltage (1400 V) was applied to the PMT and the signal was amplified by a preamplifier with a gain of 24. We measured 100,000 events with the shutter open. The signal from these events is shown by the black-line histogram. We also determined the quantity 0 PESD, or $n_0(i)$, by measuring 100,000 events with the shutter closed; this is also shown by a black-line histogram. The quantity 1 PESD, or $n_1(i)$, is shown by the shadowed histogram, and the distributions corresponding to 2 and 3 PESDs are shown by (red) solid lines. Our initial estimate of 1 PESD, obtained in Step 2 (see text), is shown in the upper left panel. The result of the first iteration in Step 4 is shown in the lower left panel, and the second and third iterations are shown in the right panels. Four iterations proved sufficient to converge the PESDs. The average signal corresponding to a single photoelectron, as obtained from Equations 7 and 8, are also indicated in each panel.

was illuminated with the shutter open, while in the second the shutter was
 95 closed. In both measurements, the signal from the PMT was integrated in
 synchronization with the LED flash event-by-event. We consider the charge
 of the integrated signal, represented by the symbol q in units of C, to be the
 intensity of the signal. By making a histogram of the measured values of q , we
 obtained the distribution of the signal. Events are counted in bins of width of
 100 Δq for each value of q . The counted value in the i th bin from the origin at
 $q = 0$ in the positive direction is represented by $n_{all}(i)$, and the i th bin in the
 negative direction is $n_{all}(-i)$. The quantity h_{ih} is the nearest integer of $q/\Delta q$,
 and the center of each bin is represented by $q(i) = i \times \Delta q$.

The total numbers of events with the shutter open and closed, respectively,
 105 are represented by N_{all} and N_{all}^{off} . The number of k -photoelectron events – i.e.,
 number of events caused by exactly k photoelectrons – is represented by N_k .
 The number of k -photoelectron events in the i th bin is $n_k(i)$ and $n^{off}(i)$ is that
 obtained with the shutter closed. With these definitions, we have

$$N_{all}^{off} = N_0^{off} = \sum_{i=-\infty}^{\infty} n^{off}(i),$$

$$N_{all} = \sum_{i=-\infty}^{\infty} n_{all}(i) = \sum_{k=0}^{\infty} N_k = \sum_{k=0}^{\infty} \sum_{i=-\infty}^{\infty} n_k(i).$$

110 The average value of k for all events is defined as $\langle k \rangle$; thus $\langle k \rangle$ is proportional
 to the brightness of the LED and to the photo-detection efficiency. It can be
 calculated from the following equation:

$$\langle k \rangle = \frac{\sum_{k=0}^{\infty} k \cdot N_k}{N_{all}}. \quad (1)$$

Since N_k follows a Poisson distribution, it can be calculated from $\langle k \rangle$ by the
 following equation:

$$N_k = N_{all} \frac{\langle k \rangle^k}{k!} e^{-\langle k \rangle}. \quad (2)$$

115 Now we can determine N_0 . Suppose that all events with $q < 0$ are just noise. Then, we can obtain the result for zero photoelectrons – i.e., 0 PESD – from the data obtained with the shutter closed. We assume that no event caused by one or more photoelectrons makes a negative signal; this yields an estimated upper limit to N_0 . Since the number of events with negative signal is negligibly small
120 compared with the statistical error of N_0 , we incorporate such negative signals into the systematic uncertainties instead of including them in the 1 PESD. This issue will be discussed further in Section 2.6. Define the quantity α to be

$$\alpha = \frac{\sum_{i=-\infty}^{-1} n_{all}(i)}{\sum_{i=-\infty}^{-1} n^{off}(i)}. \quad (3)$$

We thus obtain $N_0 = \alpha N_0^{off}$; this estimate of N_0 causes the largest systematic uncertainty in the present analysis. Similarly, $n_0(i)$ – or equivalently, 0 PESD
125 – can be estimated as $n_0(i) = \alpha n^{off}(i)$.

Now the quantity $\langle k \rangle$ can be obtained from Equation 2 by setting $k = 0$:

$$\langle k \rangle = \ln \frac{N_{all}}{N_0}. \quad (4)$$

Substituting this result into Equation 2, we obtain

$$N_k = N_{all} \frac{\langle k \rangle^k}{k!} e^{-\langle k \rangle} = \frac{\langle k \rangle^k}{k!} N_0. \quad (5)$$

With $k = 1$, we obtain $N_1 = \langle k \rangle N_0$. Therefore Equation 5 can be rewritten as

$$N_k = \frac{N_1^k}{k! N_0^{k-1}}. \quad (6)$$

That is, N_k can also be calculated for all k using N_0 . The average value of the
130 signal corresponding to one photoelectron, $\langle Q_1 \rangle$, is defined as follows:

$$\langle Q_1 \rangle = \frac{\sum_{i=-\infty}^{\infty} n_1(i) q(i)}{N_1}. \quad (7)$$

The quantity $\langle Q_1 \rangle$ can also be calculated from the average signal from all data divided by the average number of photoelectrons (i.e., $\langle Q_1 \rangle = \langle Q \rangle / \langle k \rangle$). Thus, Equation 7 can also be written in the following alternative form:

$$\langle Q_1 \rangle = \frac{\sum_{i=-\infty}^{\infty} n_{all}(i) q(i)}{\langle k \rangle N_{all}}. \quad (8)$$

Based on Equation 8, we can thus obtain $\langle Q_1 \rangle$ without first determining 1
 135 PESD; we only need to determine N_0 . Comparing the results from Equations
 7 and 8 also provides a useful check of the analysis. The gain of the PMT can
 then be obtained from $\langle Q_1 \rangle$ divided by the elementary charge and the gain of
 the preamplifier.

2.3. Estimation of 1 PESD

140 Given the value of N_0 , 1 PESD can be determined as follows:

Step 1 We first determine the distribution of signal corresponding to one or
 more photoelectrons:

$$n_{k>0}(i) = n_{all}(i) - n_0(i).$$

In this step, the initial values of $n_1(i)$ are set equal to $n_{k>0}(i)$.

Step 2 We next integrate $n_1(i)$ from $i = -\infty$ up to the bin at which the
 145 integrated value is equal to N_1 , as calculated from Equation 5. The last
 bin number for this integration is defined as j ; that is,

$$N_1 = \sum_{i=-\infty}^j n_1(i). \quad (9)$$

The value of $n_1(j)$ is adjusted so that Equation 9 is satisfied.

The bins with $i > j$ that contain one photoelectron are set to 0 (see the
 upper left panel in Figure 3):

$$n_1(i : i < j) = n_{k>0}(i), \quad n_1(i : i > j) = 0.$$

150 **Step 3** The distribution of two or more photoelectrons can be estimated from
 the superposition of $n_1(i)$. A signal with intensity $q(i)$ that is caused by
 two photoelectrons is represented by the convolution of two signals caused
 by single photoelectrons, with intensities $q(i')$ and $q(i - i')$. Therefore

the probability distribution of the signal caused by two photoelectrons, $n_2(i)/N_2$, can be represented as follows:

$$\frac{n_2(i)}{N_2} = \sum_{i'=-\infty}^{\infty} \frac{n_1(i')}{N_1} \frac{n_1(i-i')}{N_1}. \quad (10)$$

Using Equation 6, we obtain $n_2(i)$ as

$$n_2(i) = \frac{1}{2!N_0} \sum_{i'=-\infty}^{\infty} n_1(i')n_1(i-i'). \quad (11)$$

IN a similar way, we obtain the following equations:

$$n_3(i) = \frac{1}{3!(N_0)^2} \sum_{i''=-\infty}^{\infty} \sum_{i'=-\infty}^{\infty} n_1(i'')n_1(i')n_1(i-i'-i''),$$

$$n_4(i) = \frac{1}{4!(N_0)^3} \sum_{i'''=-\infty}^{\infty} \sum_{i''=-\infty}^{\infty} \sum_{i'=-\infty}^{\infty} n_1(i''')n_1(i'')n_1(i')n_1(i-i'-i''-i'''),$$

.....

As long as Equation 9 is satisfied in Step 2, these equations ensure that the total number of events caused by k photoelectrons is always correct; i.e., $N_k = \sum_{i=-\infty}^{\infty} n_k(i)$. Of course, in a real analysis, these calculations are performed over a limited range of i and k . When k is greater than 3, the calculation takes a long time, so it is impractical to conduct calculations for large k .

Step 4 The quantity $n_1(i)$ is now re-determined from $n_k(i)$ as follows (see the lower left panel in Figure 3):

$$n_1(i) = n_{all}(i) - \sum_{k=2}^{\infty} n_k(i).$$

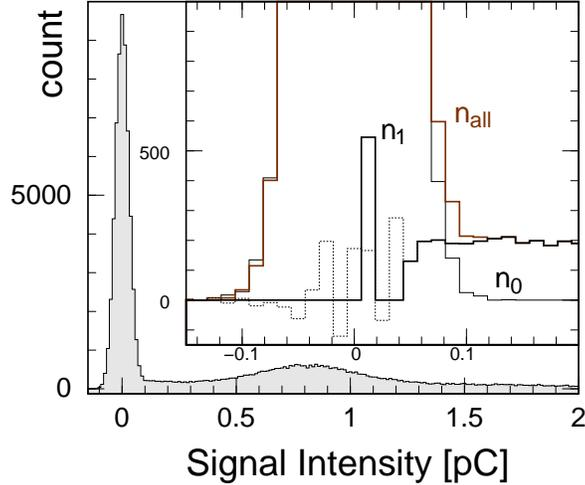


Fig. 4. The distribution of signal. The distribution around $q = 0$ is expanded in the inset panel. Both N_{all} and N_{all}^{off} are 100,000. The quantities $n_{all}(i)$, $n_0(i)$, and $n_1(i)$ are indicated by solid lines. Near the origin, we collapse the $n_1(i)$ into a single bin, as explained in Section 2.4; the distribution prior to this change is indicated by the dashed line.

Step 5 Iterate from Step 2 through Step 4 until the distributions have all converged (the right panels in Figure 3). In our analysis, we iterated these procedures four times since $\langle Q_1 \rangle$ converges to a constant value after four iterations.

170 2.4. Handling of negative bins

In the analysis of real data, the statistical error from 0 PESD is relatively large. This causes negative values of $n_1(i)$ to occur around $q = 0$. The analysis cannot deal with negative bins, and we eliminated them as follows (see Figure 4). Defining σ as the RMS width of 0 PESD, we lump all the $n_1(i)$ with $q < +1.5\sigma$ together in a single bin, with the bin number denoted by i_0 . In other words, the width of the first bin of 1 PESD is enlarged to handle its large statistical error. 175 If $n_1(i_0)$ has a negative value, we artificially set it to 0. If the negative value

is very large, this treatment produces large systematic errors. In such a case, however, there is likely to be some problem in the measurements. The charge
180 $q(i_0)$ at the center of this bin is approximately defined as

$$q(i_0) = \frac{\sum_{i=-\infty}^{1.5\sigma} n_{all}(i)q(i)}{\sum_{i=-\infty}^{1.5\sigma} n_{all}(i)}.$$

The value of $q(i_0)$ does not significantly affect the estimation of the PESDs, although $n_1(i_0)$ does make a significant contribution to the analysis, as discussed in Section 2.6. Except for $n_1(i_0)$, the values of $n_1(i)$ with $q(i) < +1.5\sigma$ are set to 0.

185 2.5. Statistical error

It is not trivial to determine the statistical error of this analysis. In this section, we first estimate the statistical error of $\langle Q_1 \rangle$ analytically from Equation 8, which we denote as $\langle Q_1 \rangle^{(8)}$. Using Equations 3 and 4, $\langle k \rangle$ can be written in the form

$$\begin{aligned} \langle k \rangle &= \ln N_{all} - \ln \alpha N^{off} \\ &= \ln N_{all} - \ln N^{off} - \ln \sum_{i=-\infty}^{-1} n_{all}(i) + \ln \sum_{i=-\infty}^{-1} n^{off}(i). \end{aligned}$$

190 With the approximation

$$\sum_{i=-\infty}^{-1} n^{off} \approx \frac{N^{off}}{2}$$

the quantity $\langle k \rangle$ becomes

$$\langle k \rangle \approx \ln \frac{N_{all}}{2} - \ln \sum_{i=-\infty}^{-1} n_{all}.$$

Substituting this into Equation 8, we obtain

$$\langle Q_1 \rangle^{(8)} = \frac{\sum_{i=-\infty}^{\infty} n_{all}(i)q(i)}{\left(\ln \frac{N_{all}}{2} - \ln \sum_{i=-\infty}^{-1} n_{all}(i) \right) N_{all}}.$$

In this equation, the only variable parameter is $n_{all}(i)$, and its error can be estimated as $\delta n_{all} = \sqrt{n_{all}(i)}$. This yields the following estimate of the error in

195 $\langle Q_1 \rangle^{(8)}$:

$$\begin{aligned}
(\delta \langle Q_1 \rangle^{(8)})^2 &= (\delta n(i))^2 \sum_{i=-\infty}^{\infty} \left(\frac{\partial \langle Q_1 \rangle^{(8)}}{\partial n_{all}(i)} \right)^2 \\
&= \frac{1}{N_{all}^2} \left(\sum_{i=-\infty}^{-1} \left(\frac{\partial}{\partial n_{all}(i)} \frac{\sum_{i'=-\infty}^{\infty} i' = -\infty n_{all}(i') q(i')}{\ln \frac{N_{all}}{2} - \ln \sum_{i'=-\infty}^{-1} n_{all}(i')} \right)^2 n(i) + \frac{\sum_{i=0}^{\infty} q(i)^2 n_{all}(i)}{(\ln \frac{N_{all}}{2} - \ln \sum_{i=-\infty}^{-1} n_{all}(i))^2} \right) \\
&= \frac{1}{(N_{all} \langle k \rangle)^2} \left(\sum_{i=-\infty}^{-1} \left(q(i) \langle k \rangle + \frac{\sum_{i'=-\infty}^{\infty} n_{all}(i') q(i')}{\sum_{i'=-\infty}^{\infty} n_{all}(i')} \right)^2 + \sum_{i=0}^{\infty} q(i)^2 n_{all}(i) \right).
\end{aligned}$$

The statistical error in $\langle Q_1 \rangle^{(7)}$ can be determined from a similar calculation, although it is more complicated. Instead, we estimate the statistical error of $\langle Q_1 \rangle^{(7)}$ by dividing the data into 10 fractions, determining the values of $\langle Q_1 \rangle^{(7)}$ for each fraction, and then estimating the error from the dispersion of these
200 quantities. In this way, the values of $\langle Q_1 \rangle$ obtained from Equations 7 and 8 are found to be

$$\begin{aligned}
\langle Q_1 \rangle^{(7)} &= 0.717 \pm 0.008 [pC], \\
\langle Q_1 \rangle^{(8)} &= 0.712 \pm 0.004 [pC].
\end{aligned}$$

The error $\delta \langle Q_1 \rangle^{(7)}$ tends to be somewhat larger than $\delta \langle Q_1 \rangle^{(8)}$. This can be explained by the fact that the uncertainty in the shape of the distribution of $n^{off}(i)$ is included in $\delta \langle Q_1 \rangle^{(7)}$. The time variation of intensity of the LED may
205 also affect this error. Note that $\langle Q_1 \rangle^{(8)}$ is consistent with $\langle Q_1 \rangle^{(7)}$ to within the statistical errors.

2.6. Systematic uncertainty

The largest systematic uncertainty in this analysis is caused by the number of low-intensity events, because the distribution around $q = 0$ is sensitive to
210 environmental effects on the measurements. For example, a small current to the shutter may cause additional pickup noise.

The effect of an incorrect estimate of N_0 can be seen in Figure 5. Since $\langle k \rangle$ depends on N_0 , the value of $\langle Q_1 \rangle$ is affected by the estimate of N_0 . As shown in Figure 5, a 3 % change in N_0 causes a 5 % shift in the value of $\langle Q_1 \rangle$ and distorts
215 the estimated 1 PPSD from the Poisson-like distribution shown in Figure 3.

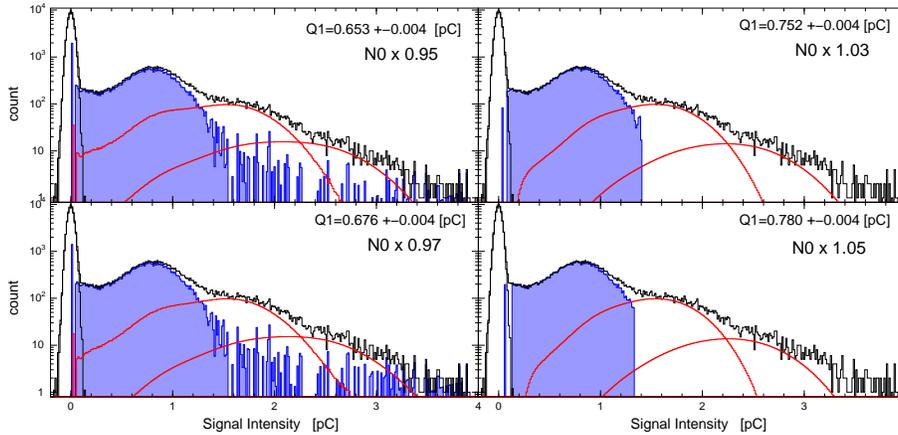


Fig. 5. Effect of a systematic shift in N_0 on the estimate of 1 PESD using the same data as in Figure 3. The value of N_0 used in Figure 3 is multiplied by 0.95, 0.97, 1.03, and 1.05 in proceeding, respectively, from the upper left to the lower right panels.

Therefore, if N_0 differs by 3 % or less, the systematic uncertainty in the value of $\langle Q_1 \rangle$ is estimated as 5 %.

Another source of systematic uncertainty is the value of $n_1(i_0)$, into which the data around $q = 0$ is collapsed (Section 2.4). While the value of $q(i_0)$ does not significantly affect the analysis, the number of events in this bin does produce a systematic uncertainty, which affects the estimate of $\langle Q_1 \rangle^{(7)}$. If this value were different by as much as 30 %, the estimate of $\langle Q_1 \rangle^{(7)}$ would only change by 3 %.

Adding these values quadratically, the systematic uncertainties in the value of $\langle Q_1 \rangle$ can thus be estimated as 6 %. Of course, this uncertainty depends on the setup of the measurements, and it may be possible to reduce it.

Additional sources of systematic uncertainty include the dark current and the after-pulse in the PMT. The dark current is mainly caused by electrons liberated by thermal fluctuations in the cathode, which are emitted randomly at a rate less than approximately 1 MHz. The after pulse is caused by secondary electrons, which are multiplied in the PMT and occasionally collide with gas

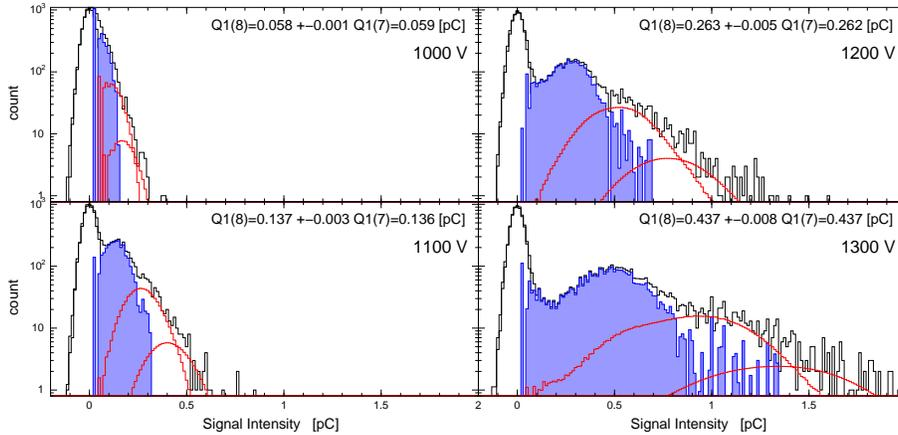


Fig. 6. Estimates of 1 PESD obtained with various PMT gains. The average signal from single photoelectrons $\langle Q_1 \rangle$, as estimated from Equations 7 and 8, are also indicated in each panel. The statistical error is inversely proportional to the square of the number of events, which is 10,000 in the measurements shown in this figure.

atoms or molecules, creating positive ions in the PMT. The positive ions are attracted to the cathode by the electric field, ejecting additional electrons that produce a relatively large signal. The rate of the after-pulse depends on the
 235 quality of the PMT; in general, there is less than a 1 % chance to produce an after-pulse by one photoelectron. These false signals can be neglected as long as the integration time is of the order of 20 ns.

3. Discussion and Summary

3.1. Discussion

240 The number of secondary electrons created at the first dynode is distributed according to a Poisson distribution. This distribution makes the largest contribution to the shape of 1 PESD. However, as can be seen in the lower right panel of Figure 3, the 1 PESD departs from a Poisson distribution at low intensity. Single-photoelectron events are increased in the low-intensity region, as com-

245 pared with a simple Poisson distribution. This can be explained by backscat-
tering of the photoelectrons at the first dynode as mentioned in Section 2.1. In
such a case, the photoelectron retains some of its energy, reducing the number
of secondary electrons that proceed to the second dynode. Consequently, the
signals from such events decrease. One of the advantages of the present analysis
250 is that these small signals are precisely included in the determination of $\langle Q_1 \rangle$
and 1 PESD.

When the gain of the PMT is small, or if the noise level is high compared with
the single-photoelectron signal, it becomes difficult to discriminate between the
1 PESD and 0 PESD signals. To test for this condition, we estimated 1 PESD
255 using several values of the high voltage on the PMT. The resulting 1 PESIDs,
corresponding to PMT gains from 10^4 to 10^5 , are shown in Figure 6. The
statistical error of the estimated $\langle Q_1 \rangle$ decreases with increasing PMT gain, as
shown in this figure, although the errors are about 2 % for all high voltages.
When the high voltage is 1000 V, the 1 PESD cannot be discriminated by eye
260 from the noise component (0 PESD). However, even in this case, both 1 PESD
and the gain of the PMT can be clearly obtained using this analysis so long as
 N_0 is determined correctly.

3.2. Summary

We have developed a procedure to estimate the average signal produced by
265 a single photoelectron, along with its distribution, which is one of the most
fundamental parameters required for measuring the intensity of weak light us-
ing a photon detector such as a PMT. In this method, we utilize the fact that
the number of photoelectrons reaching the first dynode follows a Poisson dis-
tribution. Comparing the distributions of signals from the PMT obtained with
270 the light source turned on and off (or, equivalently, with the shutter open and
closed), we can estimate the number of events with zero photoelectrons, de-
noted by N_0 . Once N_0 and the total number of events, denoted by N_{all} , are
determined, the average number $\langle k \rangle$ of photoelectrons reaching the first dynode
can be calculated uniquely from the Poisson distribution. Then the number of

275 events N_k for each number of photoelectrons can also be determined. With this
method, we can obtain the gain of the PMT and its associated error without
first determining the distribution of signal for events caused by single photo-
electrons, which we define as 1 PESD. The 1 PESD distribution can also be
estimated from the fact that a k -PESD distribution is the superposition of k
280 times the 1 PESD distribution.

Based on this method, we determined the average signal due to a single
photoelectron, $\langle Q_1 \rangle$, to within a 1 % statistical error when the gain of PMT
was 10^5 and the number of measured events was 100,000. This statistical error
is inversely proportional to the square of the number of events. Even though the
285 0 and 1 PESD distributions cannot be discriminated by eye if the gain of the
PMT is low and/or the noise level is high, the quantity $\langle Q_1 \rangle$ can be obtained,
along with its statistical error, using this method. This procedure does not
require fitting routines nor any assumptions about the shape of the 1 PESD
distribution. The shape of 1 PESD can also be determined experimentally
290 using this method. Systematic uncertainties in this analysis are mainly caused
by the determination of N_0 , which we estimated as 6 %. The most important
factor in this measurement is thus a precise measurement of 0 PESD.

The 1 PESD distribution we obtained shows that events at small signal
levels exceed the numbers expected from a Poisson distribution. As the quality
295 of PMTs improve, the detailed structure of 1 PESD will become clearer in the
measurements. Consequently, precise calibration is required to make the best
use of the quality of the detector. This requirement led to the present study.

In summary, we have developed a procedure to estimate the average signal
produced by a single photoelectron, $\langle Q_1 \rangle$, and to obtain the gain of the PMT.
300 The most important parameter turns out to be the number of events caused
by zero photoelectrons, namely noise events. Direct measurement of the signal
produced by a single photoelectron proves to be unnecessary.

Acknowledgments

The authors thank the CTA collaboration for their assistance. This work
305 is supported by JSPS KAKENHI Grant Number 24000004-01, 15K13489, and
17H06131. Furthermore, it was partly supported by the joint research program
of the Institute of Cosmic Ray Research (ICRR), University of Tokyo. The
authors thank Enago (www.enago.jp) for the English language review.

This paper has gone through internal review by the CTA Consortium.

310 References

- [1] K Hamamtsu Photonics, Photomultiplier Tubes Basics and Applications,
2007.
- [2] CTA consortium, Design concepts for the cherenkov telescope array
(arxiv:1008.3703), *Experimental Astronomy* 32 (2011) 192–316.
- 315 [3] E. B. Bellamy, B. Bellettini, J. Budagov, F. Cervelli, I. Chirikov-Zorin,
M. Incagli, D. Lucchesi, C. Pagliarone, S. Tokar, F Zetti, Absolute cali-
bration and monitoring of a spectrometric channel using a photomultiplier,
NIMA 339 (1994) 468–476.
- [4] J Sternglass, E, Backscattering of kilovolt electrons from solids, *Phys. Rev.*
320 95 (1954) 245–358.
- [5] R. Mirzoyan, E. Lorenz, On the calibration accuracy of light sensors in
atmospheric cherenkov, fluorescence and neutrino, in: 25th ICRC in Durban,
Vol. 7, 1997, p. 265.
- [6] T. Toyama, R. Mirzoyan, et al, for the CTA consortium, Novel photo multi-
325 plier tubes for the cherenkov telescope array project (arxiv:1307.5463), 33th
ICRC in Rio de Janeiro (2013).

- [7] R. Mirzoyan, D. Mueller, Y. Hanabata, J. Hose, D. Menzel, M. Takahashi, M. Teshima, T. Toyama, T. Yamamoto, Evaluation of photo multiplier tube for the cherenkov telescope array, NIMA 824 (2016) 640–641.